

Single photoelectron trapping, storage, and detection in a one-electron quantum dot

Deepak Sethu Rao, Thomas Szkopek, Hans Daniel Robinson, and Eli Yablonovitch
Department of Electrical Engineering, University of California Los Angeles, Los Angeles, California 90095

Hong-Wen Jiang
Department of Physics and Astronomy, University of California Los Angeles, Los Angeles, California 90095

(Received 24 June 2005; accepted 12 October 2005; published online 12 December 2005)

There has been considerable progress in electrostatically emptying, and refilling, quantum dots with individual electrons. Typically the quantum dot is defined by electrostatic gates on a GaAs/Al_yGa_{1-y}As modulation-doped heterostructure. We report the filling of such a quantum dot by a single photoelectron, originating from an individual photon. The electrostatic dot can be emptied and reset in a controlled fashion before the arrival of each photon. The trapped photoelectron is detected by a point contact transistor integrated adjacent to the electrostatic potential trap. Each stored photoelectron causes a persistent negative step in the transistor channel current. Such a controllable, benign, single photoelectron detector could allow for information transfer between flying photon qubits and stored electron qubits. © 2005 American Institute of Physics.
 [DOI: [10.1063/1.2134888](https://doi.org/10.1063/1.2134888)]

I. INTRODUCTION

The detection of a single photoelectron generally requires some type of gain mechanism. A mechanism has emerged recently, namely, photoconductive gain,¹ for providing the sensitivity needed for single charge detection.²⁻⁴ Indeed, the detection of a photohole is easier and more common than the detection of a photoelectron. The positive charge of a trapped photohole attracts electrons and leads to conventional positive photoconductivity. Recently, single photon detection has been demonstrated by photohole trapping in defects³ and self-assembled quantum dots² within semiconductors. The trapping of a photoelectron, on the other hand, repels current, and the signature of photoelectron trapping is the more exotic “negative photoconductivity.”¹ Photoelectron trapping has thus far been demonstrated in the microwave regime by photon-assisted tunnelling between Landau levels⁵ and in an electrostatic quantum dot⁴ with limited or no control over systematic emptying and injecting a single photoelectron. In this paper we report the trapping and detection of a single, interband photoelectron in a controllable electrostatic quantum dot.

The benefit of safely and gently trapping a photoelectron is that its spin information may be preserved. Favorable selection rules for information transfer between quantum states of photons and spin states of electrons in semiconductors have been identified.⁶ It may become possible to transfer quantum information over long distances by exchanging information between flying qubits and stationary qubits.⁷

It is essential that any optospintronic device designed to achieve the above objectives accomplishes the following tasks: (i) trap a photoexcited electron in an artificially engineered trap; (ii) detect the stored electron by means of a benign gain mechanism; and, most importantly, (iii) ensure that the trap holds none but the single photoexcited electron.

We experimentally demonstrate the injection and detection of a single, interband photoexcited electron, into an empty quantum dot defined electrostatically by metallic gates on a GaAs/AlGaAs heterostructure, with an integrated charge read-out transistor.

Negative photoconductivity is commonly not observed in GaAs/AlGaAs heterostructures, although a persistent photoinduced increase in conductivity has been well known for some time now⁸ due to an increase in the two-dimensional electron gas (2DEG) density. We have earlier reported the detection of individual photohole trapping events with a simple split-gate geometry.³ Photoholes are trapped predominantly by negatively charged defects at low temperatures known as DX centers. Persistent negative photoconductivity at low temperatures has been reported only after the saturation of hole trapping centers, most likely ionized donors, and only at short wavelengths causing photoexcitation in the doped AlGaAs barrier layer.^{9,10}

By creating an artificial electron trap defined by electrostatic metal gate electrodes, we have been able to detect the addition of a single photoexcited electron into the electron trap. We suppressed the usually dominant positive photoconductivity by a shadow mask, that permitted the light to fall only in the immediate vicinity of the electrostatic quantum dot. A Quantum Point Contact (QPC) field-effect transistor integrated adjacent to the dot¹¹ serves to detect the injected photoelectron in a nonintrusive way. As an electron is injected into the quantum dot, the increased electrostatic repulsion causes a negative conductivity step in the QPC transistor current. It is important to detect the single electron events and the trapped electric charge by means of an adjacent transistor, rather than by invasively passing current through the dot.

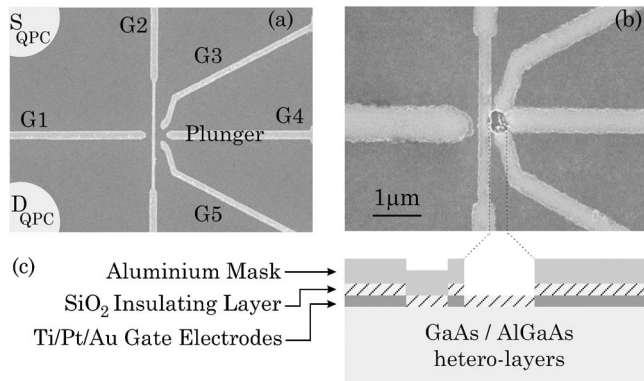


FIG. 1. (a) Scanning electron micrograph of the surface metallic gates defining a quantum point contact (QPC) between the source and drain Ohmic contacts (S_{QPC} and D_{QPC}) and a lateral electrostatic quantum dot. (b) SEM of pinhole aperture etched in an opaque Al layer, 150 nm thick, acting as a shadow mask to illuminate only the quantum dot region. Gates are buried under Al/SiO₂ layers. (c) Cross section view of the device. The GaAs/AlGaAs heterostructure consists of a 5 nm Si-doped ($1 \times 10^{18}/\text{cm}^3$) GaAs cap layer, a 60 nm Si-doped ($1 \times 10^{18}/\text{cm}^3$) $n\text{-Al}_{0.3}\text{Ga}_{0.7}\text{As}$ layer, a 30 nm $i\text{-Al}_{0.3}\text{Ga}_{0.7}\text{As}$ spacer layer, on an undoped GaAs buffer.

II. DEVICE LAYOUT

Our device is fabricated on a modulation-doped GaAs/Al_{0.3}Ga_{0.7}As heterostructure grown by molecular beam epitaxy on a semi-insulating GaAs substrate. A scanning electron micrograph of the gate geometry of the device used in our measurements is shown in Fig. 1. The gates are fabricated by electron beam lithography and electron-gun evaporation of Ti/Pt/Au. G1 and G2 define a QPC between the left source and drain Ohmic contacts, S_{QPC} and D_{QPC} , respectively, shown in Fig. 1(a). Adjacent to the QPC, an electrostatic circular quantum dot with a lithographic radius of 200 nm is defined by gates G3, G4, and G5. The electrostatic dot is defined by squeezing the 2DEG by the surface metallic gates. A variety of experiments have studied the properties of such GaAs/AlGaAs quantum dots in great detail,^{11–14} and a vast knowledge base has been developed.

Negative voltages on the five surface gates isolate a puddle of electrons in the 2DEG adjacent to the point contact transistor. Gates G3 and G5, together with G2, control the tunnel coupling of the electrons in the dot to the external 2DEG reservoirs, while gate G4 is used as a plunger to push electrons out of the dot one at a time down to the last electron. This creates an empty dot just before exposure to light. Photoevents over the bulk of the device are suppressed by a 150 nm thick aluminum layer deposited as a mask over the entire area of the device, except for a pinhole aperture directly above the quantum dot, as shown in the SEM of Fig. 1(b). An insulating SiO₂ layer and a thin adhesion layer of titanium separate the metal gate electrodes from the aluminum mask layer. Figure 1(c) shows the cross section view of the device layers.

III. EXPERIMENTAL RESULTS AND DISCUSSION

Figures 2 and 3 present the electrical characterization of the charge sensitivity of the QPC toward detecting single electron events in the adjacent quantum dot capable of storing electrons in a long-lived metastable state. The device is

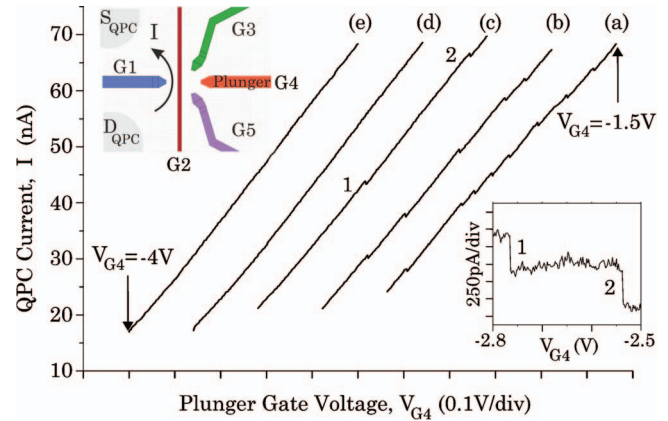


FIG. 2. (Color) Single electron escape from the dot detected by the QPC transistor. The plunger gate, G4, is swept from -1.5 V to -4 V with a scan rate of 4 mV/s starting at curve marked (a) and ending at (e) with each curve spanning 0.5 V. Gates G2, G3, and G5 are held at -0.9 V while G1 is changed in between each curve, to reset the QPC current. The curves have been offset along the voltage axis to fit on one graph. The bottom inset shows the step sizes of the last two electrons in the dot seen in curve (c) after subtracting out the background slope [$V_{\text{SD}}(\text{QPC}) = 3.25$ mV, $G_{\text{QPC}} = 0.35 e^2/h$ at the last electron step on curve (c)].

cooled gradually to 0.43 K in a ³He cryostat and negative voltages are applied to the five metallic gates defining the dot and the QPC. Figure 2 plots the current through the QPC transistor versus the plunger gate voltage, V_{G4} . The plunger is swept at a rate of 4 mV/s to repel electrons one at a time, into the surrounding 2DEG.

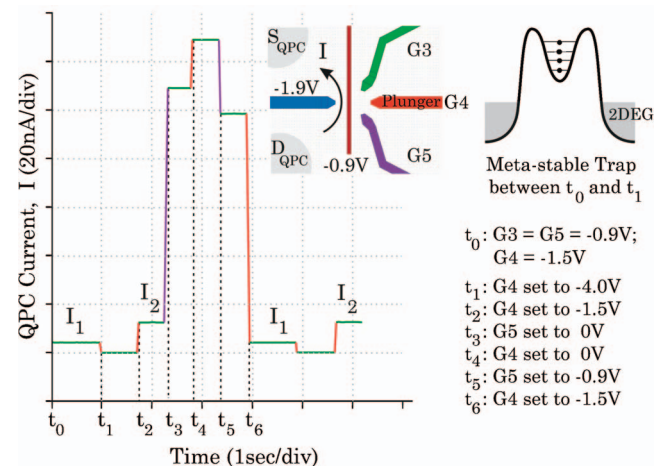


FIG. 3. (Color) Hysteresis measured in the current through the QPC transistor, associated with the transition of the dot from the metastable filled state to the equilibrium empty state. The current switches from I_1 to I_2 as the G4 plunger gate ejects stored electrons in the cycle from t_0 to t_2 . In the metastable state following t_0 (or equivalently t_6), the dot potential resides above the surrounding Fermi level, as shown in the top right inset. The thick tunnel barriers formed in our geometry when G3 and G5 are at -0.9 V prevent fast tunnelling of the trapped electrons. At t_1 , these electrons are forcibly expelled over the thick barriers by a large repulsive potential on the plunger. They do not subsequently reenter when the potential well is recreated at t_2 , owing to the thick barriers. When the barriers are reopened and closed in the cycle from t_3 to t_6 , electrons remain trapped in the dot, restoring the current to I_1 . The color of the vertical transitions is coded to the color of the corresponding gate switch for that transition. Level I_2 represents the desired empty state of the dot, at which it is ready to accept and trap photoinjected electrons. Such a hysteretic behavior in the QPC current could be observed whenever the plunger gate voltage sweep was begun at a value prior to the removal of the last electron from the dot and no hysteresis was observed upon starting from an empty dot.

The quantum dot state, at the start of the scan in Fig. 2, is the same as that at time t_0 (or equivalently t_6) in Fig. 3. Upon formation, a few excess electrons remain trapped in the dot in a long-lived metastable state, prior to being forced out by the plunger gate. The point contact current varies in a sawtooth fashion with a small discrete positive step for each electron ejected, as seen in Fig. 2. The last electron emission event occurs on curve (c) at a voltage of about $G_4 = -2.75$ V on the plunger gate. In order to ensure that the absence of further steps is not due to very slow tunnelling times, the barrier gate voltage G_3 was raised just after the last detected step to allow any remaining electrons to escape. Only a smooth increase in the QPC current could be observed due to the capacitive coupling between the point contact and the tunnel barrier gate, with no evidence for any remaining electrons. The lower inset to Fig. 2 shows the steps corresponding to the last two electrons after subtracting out the background slope. The observed single electron step sizes of about 500 pA provide an excellent signal to noise ratio.

Upon sweeping the plunger gate G_4 from -4.0 V back to -1.5 V at the same scan rate as in the forward direction, no electrons were observed to reenter the dot. This comes about when the last few electrons remain trapped at energy levels far above the Fermi level in the surrounding 2DEG, as shown schematically in the right inset to Fig. 3. Strongly isolated dots can trap electrons in a metastable state for durations exceeding tens of minutes.¹⁵ However, they may be expelled from the dot by forcibly pushing them over the tunnel barriers with a sufficiently large repulsive voltage on the plunger, and they cannot subsequently reenter.

Figure 3 illustrates the hysteretic behavior in the QPC transistor current associated with the emission of electrons from the dot. Immediately following time t_0 , and equivalently time t_6 , the dot exists in the metastable state with excess trapped electrons. No electrons were observed to escape in the interval between time t_0 and t_1 . At t_1 , the setting of gate $V_{G_4} = -4.0$ V is so extreme that it overwhelms the barriers and the well trapping potential becomes a repulsive potential forcing the electrons out within the fall time of the plunger voltage. At t_2 , the plunger potential is reset and the dot is created in the equilibrium empty state. The QPC current level I_1 corresponds to the filled metastable dot state and level I_2 to the empty state, at which the dot is ready to accept and hold only the photoinjected electron with an observed storage time $\gg 5$ min.

Highly attenuated light pulses at a vacuum wavelength $\lambda = 760$ nm, which photoexcite interband electrons in the GaAs layer, were created by a Pockels cell modulator at the output of a cw laser. The pulses were focused onto a spot size of about $100 \mu\text{m}$ diameter on the sample. The aluminum mask blocks almost all of the incident photon flux except directly above the dot, where the 200 nm radius pinhole aperture is etched. Assuming a Gaussian profile for the incident spot over the illumination area of radius $50 \mu\text{m}$, and given the 200 nm radius of the electrostatic dot, the photon flux into the dot is reduced by at least a factor of 10^{-5} compared to the total incident flux.

Figure 4, which plots the QPC transistor current versus

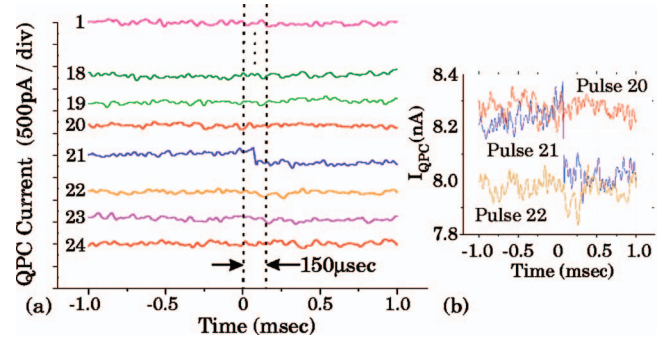


FIG. 4. (Color) (a) Photoelectron trapping in the quantum dot detected by adjacent point contact transistor. The dot is fully emptied before exposure to $\lambda = 760$ nm pulses, at a flux of 0.1 photons/pulse into the dot, within a $150 \mu\text{s}$ time window. The time traces depict the transistor current, centered on the pulse time window. The traces have been offset for clarity. (b) An expanded view of transistor current for pulses 20, 21, and 22 without any offset. The charge sensitivity per photoelectron is $10^{-3} e/\sqrt{\text{Hz}}$.

time, presents a typical experimental result of exposure to a series of consecutive pulses after emptying the dot, prior to the first pulse. In this figure, the incident photon flux was maintained at 0.1 photons/pulse within the dot area. Time $t = 0$ marks the time at which the Pockels cell was opened, for a pulse duration of $150 \mu\text{s}$. When a photon is absorbed within the active area, and the photoelectron gets trapped in the dot, a sharp drop in the transistor current is seen for pulse 21 in the series. The current step size is consistent with the expected single electron steps determined from the electrical characterization in Fig. 2. After emptying the dot by the plunger gate G_4 , if even any one of the gates G_3 , G_4 , or G_5 is grounded, the quantum dot is open and negative photoconductivity steps were not observed. We thus rule out the possibility of negative photoconductivity steps due to photoelectron trapping in donors, DX centers and traps in the SiO_2 layer. The fall time associated with the single electron signal is $20 \mu\text{s}$, from Fig. 4(b), consistent with the speed of the preamp that was used. Given the signal-to-noise ratio in Fig. 4(b), this leads to a single photoelectron signal-to-noise ratio of about 10^{-3} electrons/ $\sqrt{\text{Hz}}$.

Increasing the photon flux over the dot increases the frequency of occurrence of negative photoconductivity steps. Figure 5 shows a series of traces for a photon flux of 1.2 photons/pulse into the dot with no reset to empty the dot between pulses. Based on the frequency of occurrence of photodetection events, we estimate the photoelectron trapping quantum efficiency to be about 10%. This is consistent with the penetration depth of $\lambda = 760$ nm light, and the size of the electrostatic potential dot. Interspersed among the negative steps, some positive steps were occasionally seen, as in the 34th pulse in Fig. 5. Such positive steps, which occurred even when the gate electrodes G_3 , G_4 , or G_5 were grounded, were seen with a 1% occurrence rate and can be attributed to the photoionization of residual neutral donors close to the QPC. The occasional positive steps were more noticeable when the dot held several photoelectrons, possibly due to the additional mechanism of photoelectron ionization or photohole annihilation within the dot. The positive steps are rare since almost all the photoholes are swept away by the surrounding negatively biased gate electrodes.

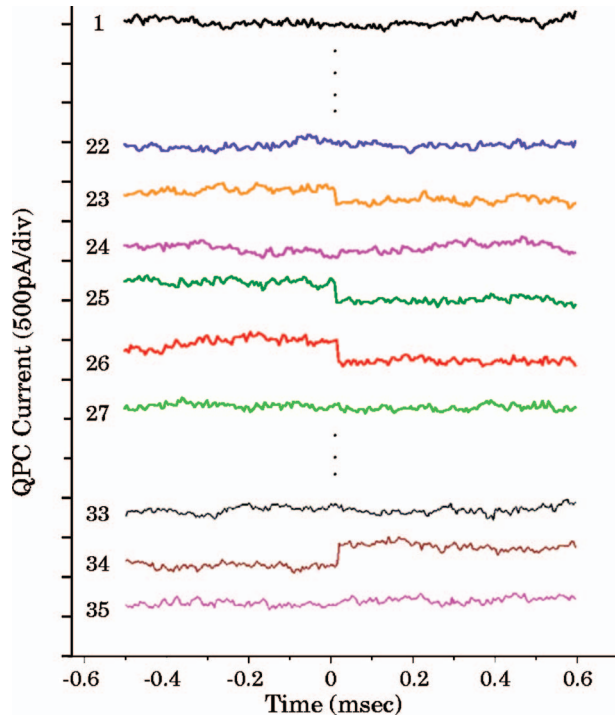


FIG. 5. (Color) An optical pulse series with an average flux of 1.2 photons/pulse within the dot area. Occasional positive steps can be attributed to the photoionization of a residual neutral donor, or the annihilation of a photohole within the electrostatic dot.

IV. CONCLUSION

In conclusion, we have demonstrated single photoelectron trapping and storage in an empty electrostatic quantum dot that can be controllably created prior to the photoexcitation of interband electrons. Recently, experiments demonstrating the electrical measurement of a single electron spin inserted in a similar electrostatic dot¹⁶ or in a commercial Si field-effect transistor¹⁷ have been reported. The successful trapping and detection of photoelectrons reported here, in spite of the usually dominant positive photoconductivity, would enable the implementation of a detector for an opti-

cally injected spin. By combining the single photoelectron trapping result reported in this paper, with the single spin measurement reported in Ref. 16, it would be possible to convert a flying qubit (photon) into a stationary qubit (trapped electron) and to measure the spin state.

ACKNOWLEDGMENTS

The work is supported by the Defense Advanced Research Projects Agency (MDA972-99-1-0017), Army Research Office (DAAD19-00-1-0172), and the Defense Microelectronics Activity.

- ¹A. Rose, *Concepts in Photoconductivity and Allied Problems* (Krieger, Huntington, NY, 1978).
- ²A. Shields, M. O'Sullivan, I. Farrer, D. Ritchie, R. Hogg, M. Leadbeater, C. Norman, and M. Pepper, *Appl. Phys. Lett.* **76**, 3673 (2000).
- ³H. Kosaka, D. S. Rao, H. D. Robinson, P. Bandaru, T. Sakamoto, and E. Yablonovitch, *Phys. Rev. B* **65**, 201307 (2002).
- ⁴H. Kosaka, D. S. Rao, H. D. Robinson, P. Bandaru, K. Makita, and E. Yablonovitch, *Phys. Rev. B* **67**, 045104 (2003).
- ⁵S. Komiyama, O. Astafiev, V. Antonov, T. Kutsuwa, and H. Hirai, *Nature* **403**, 405 (2000).
- ⁶R. Vrijen and E. Yablonovitch, *Physica E (Amsterdam)* **10**, 569 (2001).
- ⁷C. Bennett, G. Brassard, C. Crepeau, R. Jozsa, A. Peres, and W. Wootters, *Phys. Rev. Lett.* **70**, 1895 (1993).
- ⁸R. J. Nelson, *Appl. Phys. Lett.* **31**, 351 (1977).
- ⁹I. Kukushkin, K. von Klitzing, K. Ploog, V. Kirpichev, and B. Shepel, *Phys. Rev. B* **40**, 4179 (1989).
- ¹⁰J. Chen, C. Yang, R. Wilson, and M. Yang, *Appl. Phys. Lett.* **60**, 2113 (1992).
- ¹¹M. Field, C. Smith, M. Pepper, D. Ritchie, J. Frost, G. Jones, and D. Hasko, *Phys. Rev. Lett.* **70**, 1311 (1993).
- ¹²M. Ciorga, A. Sachrajda, P. Hawrylak, C. Gould, P. Zawadzki, S. Jullian, Y. Feng, and Z. Wasilewski, *Phys. Rev. B* **61**, R16315 (2000).
- ¹³D. Sprinzak, Y. Ji, M. Heiblum, D. Mahalu, and H. Shtrikman, *Phys. Rev. Lett.* **88**, 176805 (2002).
- ¹⁴J. Elzerman, R. Hanson, J. Greidanus, L. W. van Beveren, S. D. Franceschi, L. Vandersypen, S. Tarucha, and L. Kouwenhoven, *Phys. Rev. B* **67**, 161308 (2003).
- ¹⁵J. Cooper, C. Smith, D. Ritchie, E. Linfield, Y. Jin, and H. Launois, *Physica E (Amsterdam)* **6**, 457 (2000).
- ¹⁶J. Elzerman, R. Hanson, L. W. van Beveren, B. Witkamp, L. Vandersypen, and L. Kouwenhoven, *Nature* **430**, 431 (2004).
- ¹⁷M. Xiao, I. Martin, E. Yablonovitch, and H. W. Jiang, *Nature* **430**, 435 (2004).